Stark-shift-chirped rapid-adiabatic-passage technique among three states

A. A. Rangelov,[1] N. V. Vitanov,[1,2] L. P. Yatsenko,[3] B. W. Shore,[4,5] T. Halfmann,[4] and K. Bergmann[4]
[1]*Department of Physics, Sofia University, James Bourchier 5 Boulevard, 1164 Sofia, Bulgaria*
[2]*Institute of Solid State Physics, Bulgarian Academy of Sciences, Tsarigradsko Chaussée 72, 1784 Sofia, Bulgaria*
[3]*Institute of Physics, National Academy of Science of Ukraine, Prospect Nauki 46, Kiev-39, 03650, Ukraine*
[4]*Fachbereich Physik der Universität, Erwin-Schrödinger-Strasse, 67653 Kaiserslautern, Germany*
[5]*618 Escondido Circle, Livermore, California, USA*
(Received 25 July 2005; published 8 November 2005)

We show that the technique of Stark-chirped rapid adiabatic passage (SCRAP), hitherto used for complete population transfer between two quantum states, offers a simple and robust method for complete population transfer amongst three states in atoms and molecules. In this case SCRAP uses three laser pulses: a strong far-off-resonant pulse modifies the transition frequencies by inducing dynamic Stark shifts and thereby creating time-dependent level crossings amongst the three diabatic states, while near-resonant and moderately strong pump and Stokes pulses, appropriately offset in time, drive the population between the initial and final states via adiabatic passage. The population transfer efficiency is robust to variations in the intensities of the lasers, as long as these intensities are sufficiently large to enforce adiabatic evolution. With suitable pulse timings the population in the (possibly decaying) intermediate state can be minimized, as with stimulated Raman adiabatic passage (STIRAP). This technique applies to one-photon as well as multiphoton transitions and it is also applicable to media exhibiting inhomogeneous broadening; these features represent clear advantages over STIRAP by overcoming the inevitable dynamical Stark shifts that accompany multiphoton transitions as well as unwanted detunings, e.g., induced by Doppler shifts.

DOI: 10.1103/PhysRevA.72.053403 PACS number(s): 32.80.Qk, 32.80.Bx, 33.80.Be

I. INTRODUCTION

The technique of Stark-chirped rapid adiabatic passage (SCRAP), recently proposed [1] and demonstrated experimentally [2,3], provides a robust and efficient method for producing complete population transfer between two bound states of a quantum system—an initially populated ground state 1 and an excited state 2. SCRAP uses a nearly resonant pump laser pulse, which drives the population between states 1 and 2, and an intense far-off-resonance Stark laser pulse, which modifies the transition frequency by Stark shifting the energies of the two states. In brief, the procedure is as follows. The pump-laser carrier frequency is tuned slightly away from resonance with the Bohr transition frequency so that the pulsed Stark laser induces two separated crossings of the diabatic energy levels. If the pump pulse is sufficiently intense and is applied during one of these crossings, it will produce complete adiabatic passage of population from state 1 to state 2. If, in addition, the pump pulse duration is sufficiently small, it will have little or no effect during the other crossing and the population will remain in state 2 (i.e., the evolution will be diabatic during the second crossing). Thus the net result of this adiabatic-diabatic evolution scenario will be complete population transfer to the excited state 2, as demonstrated experimentally in metastable helium atoms [2].

As with other adiabatic processes, SCRAP is insensitive to small-to-moderate changes of the intensities and the carrier frequencies of the pump and Stark pulses, and to the delay between the two pulses. It is particularly important that SCRAP can be used with multiphoton as well as single-photon transitions, provided the Stark shifts induced by the pump pulse are small compared to those induced by the Stark laser [2].

The SCRAP technique can also be used to produce coherent superpositions: within appropriate ranges of carrier frequency detunings it operates as half-SCRAP [4] and prepares a persistant maximum coherent superposition of the two states. The composition of the created superposition is controlled by the detuning and is robust against variations in the other interaction parameters.

It is natural to consider the possibility of extending SCRAP from a two-state system to a three-state chain, with the aim of transferring population between the first and last states of this chain. In this respect, three-state SCRAP represents an alternative to stimulated Raman adiabatic passage (STIRAP) [5], which is a popular technique for inducing complete and robust population transfer between the end states of a Raman-type linkage. In this technique, the population is transferred adiabatically from an initially populated state 1 to a target state 3 by means of two partially overlapping pulses: a pump pulse that couples state 1 to an intermediate state 2 and a Stokes pulse that couples state 2 to the target state 3. For STIRAP the Stokes pulse occurs first (i.e., counterintuitive ordering), placing the system into an adiabatic state that does not involve the intermediate state 2—a dark state or population trapping state [6]. The dark state provides an adiabatic route from the initial state 1 to the target state 3. Population remains trapped in this particular adiabatic state so long as the time evolution remains adiabatic and the condition of two-photon resonance between states 1 and 3 is maintained. Because STIRAP is based on adiabatic evolution, it is insensitive to pulse shapes and pulse areas and it is therefore robust.

Successful implementation of STIRAP requires two-photon resonance. When dynamic Stark shifts are present, as occurs when the pump and/or Stokes linkages are by two-

photon or multiphoton transitions, then the overall (two-photon or multiphoton) detuning changes with time, and special care is required to produce successful population transfer [7,8].

We here consider using SCRAP to overcome the detrimental effects of the Stark shifts induced by the pump and Stokes lasers. In fact, SCRAP uses (controlled) Stark shifts to an advantage: they create a set of level crossings in the energy diagram of the system, which are then manipulated by properly timed laser pulses in order to design an adiabatic route from state 1 to state 3. Because three-state SCRAP does not require maintaining an exact resonance, it is expected to be much more robust against unwanted Stark shifts than STIRAP and hence, to offer a powerful alternative tool for adiabatic population transfer, at least when multiphoton transitions and inhomogeneous broadenings are involved.

This paper is organized as follows. In Sec. II we provide some basic definitions and equations, distinguish adiabatic and diabatic evolution, and present the fundamentals of two-state SCRAP. In Sec. III we introduce and analyze three-state SCRAP and derive the general conditions on the interaction parameters: detunings, pulse timings, Rabi frequencies and Stark shifts. In Sec. IV we display various numerical examples of the dependence of three-state SCRAP on the experimental parameters and verify the derived analytic conditions. In Sec. V we compare SCRAP and STIRAP. Finally, Sec. VI summarizes our observations concerning this technique.

II. BACKGROUND

A. Basic definitions and equations

We are concerned with calculating the time dependent probabilities $P_k(t)$ for finding the system in state k at time t, given that it was initially prepared in state $k=1$ and was subsequently subjected to various pulsed interactions. Specifically, for the three-state system, we wish to maximize the final population $P_3 \equiv P_3(\infty)$ of the target state 3, having begun with population entirely in state 1. Because our concern is with coherent excitation we deal with dynamics governed by the time-dependent Schrödinger equation. Using this equation, we will describe population losses out of the system by spontaneous emission by introducing complex detunings. We use the traditional rotating-wave picture [and rotating-wave approximation (RWA) [9]] for defining probability amplitudes $C_k(t)$ such that $P_k(t)=|C_k(t)|^2$; these satisfy the time-dependent Schrödinger equation

$$i\hbar \frac{d}{dt}\mathbf{C}(t) = \mathsf{H}(t)\mathbf{C}(t), \tag{1}$$

where $\mathbf{C}(t)=[C_1(t),\ldots,C_N(t),\ldots]^T$ is a column-vector of probability amplitudes for the N-state system of interest. In the case of a two-state system, such as is needed for SCRAP, the RWA Hamiltonian is given by [9]

$$\mathsf{H}(t) = \hbar \begin{bmatrix} 0 & \frac{1}{2}\Omega(t) \\ \frac{1}{2}\Omega(t) & \Delta(t) \end{bmatrix}. \tag{2}$$

Here the laser-induced coupling between the states is quantified by the Rabi frequency $\Omega(t)$, whose time dependence derives from that of the pump-laser electric-field amplitude $\mathcal{E}(t)$. For single-photon electric-dipole transitions $\Omega(t)$ is proportional to $\mathcal{E}(t)$. For two-photon transitions $\Omega(t) \propto |\mathcal{E}(t)|^2$, i.e., to the laser intensity.

The detuning $\Delta(t)$ is the offset of the pump-laser carrier frequency ω_p (for a single-photon transition) from the atomic Bohr transition frequency $\omega_a=(E_2-E_1)/\hbar$, possibly shifted by dynamic Stark effects

$$\Delta(t) = \omega_a - \omega_p + S_2(t) - S_1(t). \tag{3}$$

The dynamic Stark shift $S_k(t)$ of state k ($k=1,2$) originates with both the pump and Stark fields

$$S_1(t) = S_1^p f_p(t) + S_1^s f_s(t), \tag{4a}$$

$$S_2(t) = S_2^p f_p(t) + S_2^s f_s(t), \tag{4b}$$

where the dimensionless functions $f_p(t)$ and $f_s(t)$ are the envelopes of the pump and Stark laser intensities (i.e., absolute squares of electric field amplitudes), while S_k^x ($k=1,2$; $x=p,s$) are the maximum Stark shifts. The detuning can be written as the difference $\Delta(t)=\Delta_0-S(t)$ between the static detuning of the pump field from the Bohr frequency of the atom in the absence of radiation $\Delta_0=\omega_a-\omega_p$, and the difference of the Stark shifts of states 1 and 2, i.e., the net detuning Stark shift $S(t) \equiv S_1(t)-S_2(t)$. Because the Stark shifts of the ground and excited states are different [usually $|S_1(t)| \ll |S_2(t)|$], the detuning (3) is also Stark shifted.

The Stark shifts induced by the pump laser can be significant for multiphoton transitions but are negligible for single-photon transitions. For simplicity we will assume initially that these shifts can be neglected compared with those induced by the Stark field; then

$$S(t) = S_1(t) - S_2(t) \approx S_0 f_s(t), \tag{5}$$

with $S_0=S_1^s-S_2^s$.

B. Adiabatic and diabatic evolution

The state vector $\Psi(t)$ describing an N-state system moves within an N-dimensional Hilbert space, meaning it can be specified using coordinates oriented along any N independent vectors. Two choices for these coordinates prove particularly useful. The two-state Hamiltonian of Eq. (2) appears in a basis of diabatic (or "bare") states ψ_1 and ψ_2; the diagonal elements of this matrix are the diabatic energies 0 and $\hbar\Delta(t)$. An alternative choice is afforded by the time dependent adiabatic states $\Phi_+(t)$ and $\Phi_-(t)$, defined at each time t through the eigenvalue equation $\mathsf{H}(t)\Phi_\mu(t)=\hbar\varepsilon_\mu(t)\Phi_\mu(t)$, ($\mu=+,-$). The two eigenstates for $N=2$ can be expressed as

$$\Phi_+(t) = \sin\vartheta(t)\psi_1 + \cos\vartheta(t)\psi_2, \tag{6a}$$

$$\Phi_-(t) = \cos\,\vartheta(t)\psi_1 - \sin\,\vartheta(t)\psi_2, \tag{6b}$$

where $\tan 2\vartheta(t) = \Omega(t)/\Delta(t)$. This transformation produces the adiabatic Hamiltonian

$$\mathsf{H}^a(t) = \hbar \begin{bmatrix} \varepsilon_-(t) & -i\dot{\vartheta}(t) \\ i\dot{\vartheta}(t) & \varepsilon_+(t) \end{bmatrix}, \tag{7}$$

governing the evolution of probability amplitudes in the adiabatic basis. Here $\hbar\varepsilon_\pm(t)$ are the eigenvalues of the Hamiltonian (2), where

$$\varepsilon_\pm(t) = \frac{1}{2}[\Delta(t) \pm \varepsilon(t)] \tag{8}$$

and

$$\varepsilon(t) = \sqrt{\Omega^2(t) + \Delta^2(t)} = \varepsilon_+(t) - \varepsilon_-(t) \tag{9}$$

is the eigenvalue splitting. Two extreme situations are of interest, in each of which the state vector $\Psi(t)$ appears fixed in a coordinate system.

Diabatic time evolution occurs when the state vector $\Psi(t)$ remains in the same diabatic state(s), with no change in the probabilities $P_k(t)$. In the most trivial case, diabatic evolution takes place when there is no coupling between the diabatic states, i.e., when $\Omega(t) \approx 0$.

Adiabatic evolution occurs when the state vector $\Psi(t)$ remains, apart from varying phases, in a fixed superposition of adiabatic states: there will be no change in the populations of the adiabatic states but changes can occur in the diabatic populations $P_k(t)$ if the adiabatic basis is nonstationary. For example, this occurs if the compositions of the adiabatic states $\Phi_-(t)$ and $\Phi_+(t)$ change, as will happen with any change in $\vartheta(t)$, e.g., when $\Delta(t)$ or/and $\Omega(t)$ change. In particular, adiabatic evolution requires that the nonadiabatic coupling $\dot{\vartheta}(t)$ is negligible compared to the separation of the adiabatic energies

$$|\dot{\vartheta}(t)| \ll \varepsilon(t), \tag{10}$$

If the evolution is adiabatic and if the state vector $\Psi(t)$ initially coincides with one of the adiabatic states, it will remain in this single adiabatic state for subsequent times.

The concept of adiabatic evolution is particularly useful when time variation of detuning causes the diabatic energies 0 and $\hbar\Delta(t)$ to cross—a so-called level-crossing of diabatic energies. At the moment of crossing, say $t=t_c$, the detuning vanishes, $\Delta(t_c)=0$. By contrast, the adiabatic energies at this moment differ by $\hbar\varepsilon(t_c)=\hbar|\Omega(t_c)|$ and thus a plot of adiabatic energies will exhibit an avoided crossing, so long as the Rabi frequency $\Omega(t_c)$ is nonzero. As the detuning sweeps through this resonance at t_c the construction of the adiabatic states reverses: the composition of each adiabatic state is dominated by a different diabatic state before and after the crossing. Hence in the adiabatic limit, complete population transfer will occur between the diabatic states.

C. Two-state SCRAP

The mechanism of SCRAP can be understood by viewing a plot of the diabatic and adiabatic energies as a function of time, see Fig. 1. As time progresses, the Stark pulse shifts the diabatic energy of state 2 relative to that of state 1, which is taken as the fixed zero point: this detuning $\Delta(t)$ varies from Δ_0 first in one direction as the Stark pulse intensity increases, and then, as the pulse subsides, in the other direction back towards Δ_0. By appropriate choice of the carrier frequency, i.e., the static detuning Δ_0, we can make the two diabatic energies cross twice—first during the rise and then during the fall of the Stark pulse. For definiteness we assume that $S_0>0$; then for level crossings to occur, the initial static detuning Δ_0 must be in the range $0<\Delta_0<S_0$.

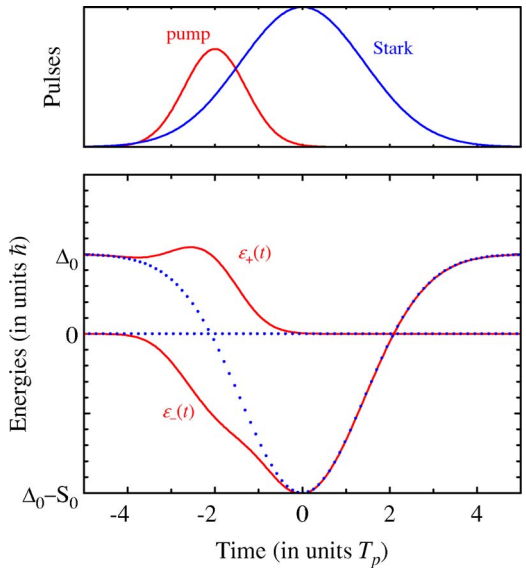

FIG. 1. (Color online) Top: Time dependences of the pump pulse and the Stark shift. Bottom: Adiabatic (solid lines) and diabatic (dotted lines) energies versus time.

If the timing of the pulses is such that the pump pulse is sufficiently strong at both crossings, e.g., if the pump and Stark pulses coincide in time, then adiabatic evolution will occur at *both* crossings. Such a pulse timing would drive the population first from state 1 into state 2 and then back into state 1—an undesired result in the present context. The success of SCRAP in producing population transfer comes from using delayed pulses, such that the pump Rabi frequency is appreciable at only *one* of the crossings. For definiteness, let us assume that the pump pulse is present only during the rising portion of the Stark pulse. Then the system, starting initially from state 1, evolves adiabatically through the first crossing, following the adiabatic state $\Phi_-(t)$, and thus makes a transition to state 2. At the second crossing there is almost no pump laser field present and hence the system evolves diabatically, following the diabatic state 2, with which it is associated prior to this crossing. The net result of this adiabatic-diabatic evolution scenario is complete population transfer from state 1 to state 2.

III. THREE-STATE SCRAP

A. Sequential double-SCRAP

The most obvious extension of SCRAP to three states is by two consecutive SCRAPs: first from state 1 to state 2 and

then from state 2 to state 3. Such a procedure corresponds to the sequence of transitions

$$\Psi(-\infty)=\psi_1 \xrightarrow{\text{SCRAP1}} \psi_2 \xrightarrow{\text{SCRAP2}} \psi_3=\Psi(\infty). \tag{11}$$

The disadvantage of this scenario is that state 2 receives the entire population between the two steps. Hence to avoid appreciable population loss by spontaneous emission from state 2, both SCRAP processes must be completed in a time shorter than the lifetime of state 2.

We will show in the following section that alternative pulse sequences, resulting in a genuine three-state SCRAP process, do not suffer from this limitation. In this process all three states are coupled during the population transfer, which offers considerably more flexibility than two sequential SCRAP processes. As with elementary two-state SCRAP, we need a diabatic-adiabatic evolution scenario for population transfer.

B. The three-state Hamiltonian

The RWA Hamiltonian of the laser-excited three-state system is expressible as

$$\mathsf{H}(t)=\hbar\begin{bmatrix} 0 & \frac{1}{2}\Omega_p(t) & 0 \\ \frac{1}{2}\Omega_p(t) & \Delta_2+S_{21}(t)-\frac{1}{2}i\Gamma & \frac{1}{2}\Omega_s(t) \\ 0 & \frac{1}{2}\Omega_s(t) & \Delta_3+S_{31}(t) \end{bmatrix}, \tag{12}$$

where $\Omega_p(t)$ and $\Omega_s(t)$ are Rabi frequencies associated with the pump and Stokes fields, respectively. The imaginary term $-(1/2)i\Gamma$ in the Hamiltonian (12) describes possible population loss from state 2 out of the system (due to spontaneous emission, ionization, etc.) at a rate Γ.

The constants Δ_2 and Δ_3 represent the static detunings, which for one-photon transitions are given by

$$\hbar\Delta_2=E_2-E_1-\hbar\omega_p, \tag{13}$$

$$\hbar\Delta_3=E_3-E_1-\hbar\omega_p+\hbar\omega_s. \tag{14}$$

The detuning shifts

$$S_{mn}(t)=S_m(t)-S_n(t), \tag{15}$$

are the differences between the Stark shifts $S_m(t)$ and $S_n(t)$ of states m and n $(m,n=1,2,3)$. Usually, the Stark shifts of the excited states are much greater than those of the ground and metastable states; hence we assume that

$$|S_2(t)| \gg |S_1(t)|, \quad |S_3(t)|. \tag{16}$$

For simplicity, we neglect at the moment the Stark shifts of states 1 and 3; hence $S_{21}(t)\approx S_2(t)$ and $S_{31}(t)\approx 0$. We shall discuss the effect of the Stark shifts $S_1(t)$ and $S_3(t)$ in Sec. V.

Underlying this assertion is the expectation that there are no near resonances of single-photon transitions that contribute to the Stark shifts. Should such resonances be present, as they have been in some instances [10], the shifts can become significant, but this is not the general case. Usually it is possible to have strong interaction on one-photon transitions without strong Stark shifts (as the latter are effects of higher order in the laser electric field).

Without loss of generality we shall assume that the Stark shift $S_2(t)$ is negative,

$$S_2(t)=-S(t)<0. \tag{17}$$

Hence the Hamiltonian (12) reads

$$\mathsf{H}(t)=\hbar\begin{bmatrix} 0 & \frac{1}{2}\Omega_p(t) & 0 \\ \frac{1}{2}\Omega_p(t) & \Delta_2+S_2(t)-\frac{1}{2}i\Gamma & \frac{1}{2}\Omega_s(t) \\ 0 & \frac{1}{2}\Omega_s(t) & \Delta_3 \end{bmatrix}. \tag{18}$$

The eigenvalues $\hbar\varepsilon_n(t)$ of the Hamiltonian (18) are roots of a cubic equation and are too cumbersome to be presented here. The corresponding eigenstates (for $k=1,2,3$) can be written as

$$\Phi_k(t)=\frac{1}{N_k(t)}\begin{bmatrix} [\varepsilon_k(t)-\Delta_3]\Omega_p(t) \\ 2\varepsilon_k(t)[\varepsilon_k(t)-\Delta_3] \\ \varepsilon_k(t)\Omega_s(t) \end{bmatrix}, \tag{19}$$

where $N_k(t)$ is a normalization factor. For specific results in simulations we shall assume Gaussian shapes for all pulses, and will take the pump and Stokes Rabi frequencies to have identical peak values Ω_0,

$$\Omega_p(t)=\Omega_0 e^{-(t-\tau_p)^2/T_p^2}, \tag{20a}$$

$$\Omega_s(t)=\Omega_0 e^{-(t-\tau_s)^2/T_s^2}, \tag{20b}$$

$$S(t)=S_0 e^{-t^2/T^2}. \tag{20c}$$

The center of the Stark pulse defines the time $t=0$. Relative to this, the pump and Stokes pulses peak at times τ_p and τ_s, respectively. In our numerical simulations we take the pump and Stokes durations equal, $T_p=T_s$, and use T_p as the unit of time and $1/T_p$ as the unit of frequency. We assume that the Stark pulse has twice this duration, $T=2T_p$, following an earlier conclusion for simple SCRAP that the Stark pulse should be longer than the driving pulse [1,2,4].

Our analysis will follow three steps. First, we shall identify the conditions for the appearance of level crossings. Second, we shall identify the timings of the pulses so that an adiabatic path linking states 1 and 3 is created. Third, we shall find the conditions under which the unwanted population of the intermediate state 2 is minimized.

C. Eigenenergies and conditions for diabatic level crossings

The first crucial condition for designing an adiabatic path between states 1 and 3 is to *create* a set of level crossings of

the diabatic energies of the three states. Because we neglect their Stark shifts the energies of states 1 and 3 are constant, see Eq. (18). These states can be linked adiabatically only if the varying energy of state 2, forced by the Stark shift $S_2(t)$, crosses both the energies of 1 and 3. For such level crossings to occur, as can be seen from Eq. (18) and condition (17), we must have

$$S_0 > \Delta_2 > 0, \tag{21a}$$

$$S_0 > \Delta_2 - \Delta_3 > 0. \tag{21b}$$

Condition (21a) ensures that the diabatic energies of states 1 and 2 cross, whereas condition (21b) ensures the crossing of the energies of states 2 and 3. If these conditions are satisfied, then there are four level crossings. For Gaussian pulses (20) the energies of states 1 and 2 cross at times $t_{12}^{\pm}=\pm t_{12}$, and those of states 2 and 3 cross at times $t_{23}^{\pm}=\pm t_{23}$, with

$$t_{12} = T\sqrt{\ln(S_0/\Delta_2)}, \tag{22a}$$

$$t_{23} = T\sqrt{\ln[S_0/(\Delta_2 - \Delta_3)]}. \tag{22b}$$

We can therefore move the crossing points along the time axis by varying the laser carrier frequencies (entering through Δ_2 and Δ_3) and the peak Stark shift S_0.

It follows from Eqs. (22) that $t_{12} > t_{23}$ for

$$0 > \Delta_3 > \Delta_2 - S_0 \tag{23a}$$

and $t_{23} > t_{12}$ for

$$\Delta_2 > \Delta_3 > 0. \tag{23b}$$

We shall see below that these two cases (23a) and (23b) lead to significant differences.

D. Pulse timings and connectivity between states 1 and 3

We assume that conditions (21) are satisfied, i.e the energy of state 2 crosses the (parallel) energies of states 1 and 3. Given these crossings, the connectivity between states 1 and 3 depends upon the timings of the pump, Stokes and Stark pulses. It is obvious that these three pulses cannot have the same time dependence because then symmetry will prevent complete adiabatic passage, as for two-state SCRAP [1,2]. Hence there must be some delays between the three pulses; however, the optimal choice of these delays is not immediately obvious. We consider three timings of the pump and Stokes pulses.

1. Intuitively ordered pump and Stokes pulses (pump-Stark-Stokes)

Figure 2 displays the time evolutions of the three pulse envelopes and the adiabatic eigenenergies for situations wherein the pump and Stokes pulses are well separated from each other but they each overlap a longer Stark pulse. Reading the figures from left to right we follow a description of intuitive pulse ordering (i.e., pump pulse occurs before Stokes), while reading from right to left we observe the pulses in counterintuitive ordering. The middle and bottom

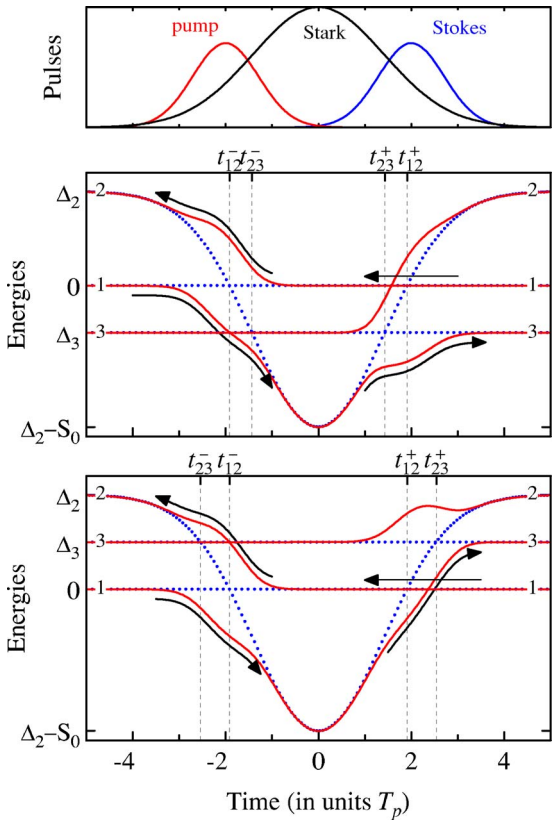

FIG. 2. (Color online) Time evolutions of the pump, Stokes and Stark pulse envelopes (upper frames), and the diabatic (dotted) and adiabatic (solid) energies of the Hamiltonian (18) (in units $\hbar$). The diabatic and adiabatic energies are plotted in two cases. Middle frame: for detunings satisfying condition (23a), with $\Delta_3=-\Delta_2/2$. Lower frame: for detunings satisfying condition (23b), with $\Delta_3=\Delta_2/2$. Arrows started from the left show time evolution of the energies for intuitively ordered pulses (pump-Stark-Stokes). Arrows started from the right show time evolution for counterintuitively ordered pulses (Stokes-Stark-pump). The other parameters are $S_0=2.5\Delta_2$, $\Omega_0=\Delta_2$, $\tau_p=-\tau_s=-2T_p$, $T=2T_p$, $T_s=T_p$.

frames show evolutions for two different orderings of the static detunings Δ_2 and Δ_3, as described by Eqs. (23a) and (23b).

For intuitive pulse ordering (pump-Stark-Stokes) both cases (23a) and (23b) permit adiabatic paths connecting states 1 and 3. For the middle frame, case (23a), this path first goes adiabatically from state 1 to state 2 through the crossing at t_{12}^-. It then follows state 2 on to an adiabatic crossing with state 3 at t_{23}^+ to end finally in state 3. The early crossing at t_{23}^- and the late crossing at t_{12}^+ are irrelevant because there is no field coupling the states whose energies cross. Similar conclusions apply for the display of the lower frame, case (23b): the adiabatic path from state 1 to 3 has an analogous structure, proceeding from state 1 to 2 to 3.

In both cases (23a) and (23b), the adiabatic path from 1 to 3 coincides with the intermediate state 2 during the middle part of the process. Thus state 2 receives almost the entire population for some time. Hence the pump-Stark-Stokes pulse ordering represents a more compact version, with a single Stark pulse, of sequential-double-SCRAP, but it is still vulnerable to decay from state 2.

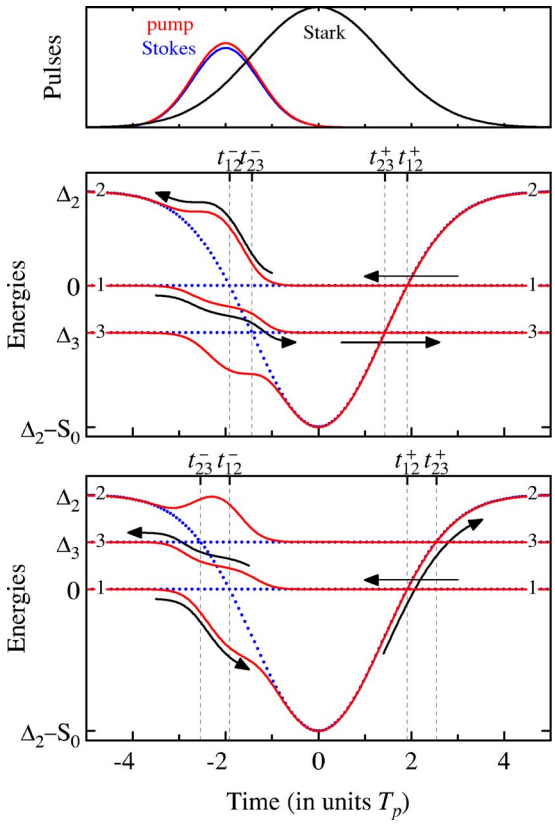

FIG. 3. (Color online) As in Fig. 2 but for coincident pump and Stokes pulses. Arrows from left to right show evolution when the pump and Stokes pulses precede the Stark pulse; arrows from the right show evolution when the Stark pulse occurs first.

2. Counterintuitively ordered pump and Stokes pulses (Stokes-Stark-pump)

By reading Fig. 2 from right to left, one can understand the time evolution when the pulse order is counterintuitive (Stokes-Stark-pump). In the absence of the Stark pulse, and with appropriate overlap of Stokes and pump pulses together with two-photon resonance, this would be an example of the STIRAP process; it would produce complete population transfer. However, in the present circumstances, with dynamic Stark shifts, this pulse ordering is inappropriate because in both cases (23a) and (23b) the initial state 1 connects to state 2 as the final state, not to the desired target state 3. The reason is evident: population changes occur only during the pump pulse. Even with a smaller delay between the pump and Stokes (i.e. for larger overlap) than the one shown in Fig. 2, the desired population transfer fails.

3. Coincident pump and Stokes pulses

When the pump and Stokes pulses act simultaneously but precede or follow the Stark pulse, as shown in Fig. 3, the two cases (23a) and (23b) produce different population evolutions.

Figure 3, read from left to right, shows the evolution when simultaneous pump and Stokes pulses occur *before* the Stark pulse. For the bottom frame, case (23b), state 1 connects finally to state 2 because the 2-3 crossing t_{23}^- occurs before the 1-2 crossing t_{12}^-; the later crossings t_{12}^+ and t_{23}^+ are irrelevant because there are no coupling fields at those times. However, for case (23a), displayed in the middle frame, the 1-2 crossing t_{12}^- is before the 2-3 crossing t_{23}^- and thus state 1 connects finally to state 3. Moreover, as evident from Fig. 3, this adiabatic path coincides only for an instant with state 2, which therefore receives at most only a small transient population during the population transfer from 1 to 3. This important feature, which is very reminiscent of STIRAP, will be discussed in more detail below.

Figure 3, read from right to left, shows the evolution when simultaneous pump and Stokes pulses occur *after* the Stark pulse. This situation leads to similar conclusions as those just mentioned, with the difference that it is now case (23b) (bottom frame) which leads to adiabatic connection from state 1 to state 3, whereas for case (23a) state 1 connects to state 2.

4. Discussion

The several illustrations discussed above are representative of many specific simulations; the qualitative picture of curve crossings and population transfers is unchanged by small variations of the pulse timings and the other parameters. From examining these figures we can identify the conditions (on pulse timings and static detunings), for which a true three-state SCRAP process can occur, i.e., a process which involves all three states and cannot be interpreted as two sequential two-state SCRAP processes. In each case there is an adiabatic path between states 1 and 3—adiabatic-transfer (AT) state—which involves only a small contribution from the (lossy) state 2. This process can occur in the following cases: case I, the detunings satisfy condition (23a) and the pump and Stokes pulses both arrive during the *rising* of the Stark pulse; case II, the detunings satisfy condition (23b) and the pump and Stokes pulses both arrive during the *falling* of the Stark pulse. Hence for fixed detunings, unlike two-state SCRAP, in three-state SCRAP the application of the driving pulses (pump and Stokes) before or after the Stark pulse leads to different results.

Successful population transfer requires appropriate settings for the interaction parameters: the timing of the pump and Stokes pulses relative to each other and to the Stark pulse, the settings of the static detunings (adjusted through the carrier frequencies of pump and Stokes pulses), and the strengths of the peak Rabi frequencies and the peak Stark shift. The following sections discuss the choice of these parameters, with figures that illustrate their relationship to needed adiabatic-diabatic crossing scenarios. We also discuss the conditions which minimize the transient population of state 2 and the ensuing population losses.

E. Adiabatic and diabatic conditions

The three-state SCRAP, similar to the original two-state SCRAP, uses a diabatic-adiabatic population transfer scenario: the path between the initial state 1 and the target final state 3 requires that certain crossings have to be passed adiabatically, others diabatically; hence we shall impose conditions for diabatic or adiabatic evolution as appropriate at each crossing.

We derive the adiabatic and diabatic conditions from the Landau-Zener formula [11]

$$P = 1 - \exp\left[- \frac{\pi \Omega^2(t_c)}{2|\dot{\Delta}(t_c)} \right] \tag{24}$$

for the probability of a transition between two diabatic states, whose energies cross at time t_c. Here $\Omega(t)$ is the coupling between them, and $\dot{\Delta}(t)$ is the detuning slope, both of which are evaluated at time t_c.

For case I, when the detunings satisfy condition (23a) and the pump and Stokes pulses precede the Stark pulse, three-state SCRAP requires adiabatic evolution during the crossings at t_{12}^- and t_{23}^-, i.e., transition probability $P > 1-\nu$, and diabatic evolution during the crossings at t_{12}^+ and t_{23}^+, i.e., transition probability $P < \nu$, where ν is a small positive number measuring the deviation from perfect adiabatic transfer. Hence the adiabatic conditions at t_{12}^- and t_{23}^-, giving lower limits on Ω_0, read

$$\frac{(\Omega_0 T)^2 \exp[-2(t_{12}+\tau_p)^2/T_p^2]}{2\Delta_2 t_{12}} > \frac{2}{\pi} \ln \frac{1}{\nu}, \tag{25a}$$

$$\frac{(\Omega_0 T)^2 \exp[-2(t_{23}+\tau_s)^2/T_s^2]}{2(\Delta_2-\Delta_3) t_{23}} > \frac{2}{\pi} \ln \frac{1}{\nu}, \tag{25b}$$

where t_{12} and t_{23} are given by Eqs. (27). The diabatic conditions at t_{12}^+ and t_{23}^+, giving upper limits on Ω_0, are

$$\frac{(\Omega_0 T)^2 \exp[-2(t_{12}-\tau_p)^2/T_p^2]}{2\Delta_2 t_{12}} < \frac{2}{\pi} \ln \frac{1}{1-\nu}, \tag{26a}$$

$$\frac{(\Omega_0 T)^2 \exp[-2(t_{23}-\tau_s)^2/T_s^2]}{2(\Delta_2-\Delta_3) t_{23}} < \frac{2}{\pi} \ln \frac{1}{1-\nu}. \tag{26b}$$

Similar conditions can be derived for case II, when the detunings satisfy condition (23b) and the pump and Stokes pulses follow the Stark pulse, with appropriate redefinition of diabatic and adiabatic crossings.

F. Minimization of the transient population of state 2

Figure 4 provides examples of the effects of slight alteration of the pump-Stokes pulse timings for case I, when the detunings satisfy condition (23a) and the pump and Stokes pulses both precede the Stark pulse. As seen in the middle frames, and as follows from Eqs. (22), the crossing between states 1 and 2 at time t_{12}^- occurs before the crossing between states 2 and 3 at t_{23}^-. One may naively expect that the best timing is to apply the pump pulse at the crossing t_{12}^- and the Stokes pulse at the crossing t_{23}^-. However, as the figure demonstrates, this choice is not the optimal one, if we wish to minimize the transient population of the lossy state 2. Indeed, for such an "intuitive" timing (left frames) state 2 receives more population than in the other two cases, of coincident pulses (middle frames) and "counterintuitive" timing (right frames). In fact, it is the "counterintuitive" timing, when the pump pulse is applied at the crossing t_{23}^- and the Stokes pulse at the crossing t_{12}^-, which produces minimum transient population of state 2.

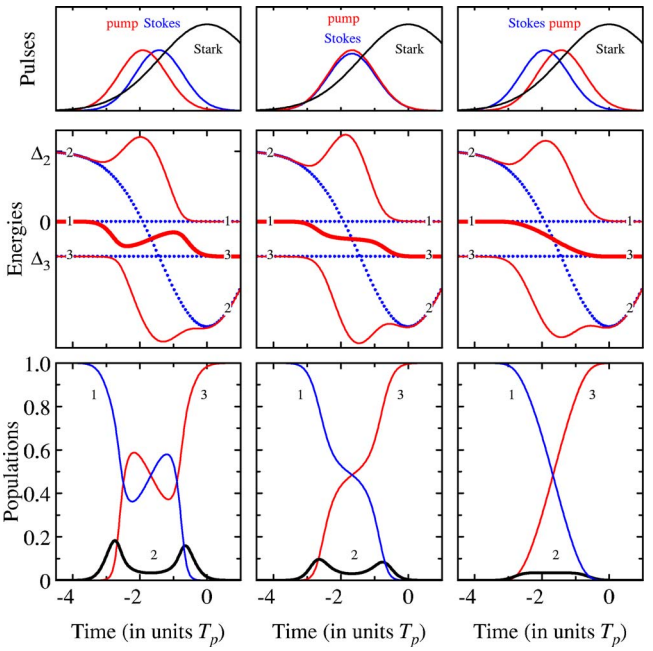

FIG. 4. (Color online) Time evolutions of the pulses (upper frames), the diabatic (dotted) and adiabatic (solid) energies of the Hamiltonian (18) (in units $\hbar$, middle frames), and the populations of the diabatic states (lower frames). Three different timings of the pump and Stokes pulses, both preceding the Stark pulse, are shown: Left frames: $\tau_p = t_{12}^-$; $\tau_s = t_{23}^-$; Middle frames: $\tau_s = \tau_p = (t_{12}^- + t_{23}^-)/2$; Right frames: $\tau_p = t_{23}^-$; $\tau_s = t_{12}^-$. The other parameters are $\Delta_3 = -\Delta_2/2$, $S_0 = 2.5\Delta_2$, $\Omega_0 = 2\Delta_2$, $T = 2T_p$, $T_s = T_p$. The thick curves in the energy (middle) frames show the AT state, which connects states 1 and 3. The populations (lower frames) are calculated in the adiabatic limit as the squared components of the AT state.

The explanation of this important result can be found in the behavior of the eigenenergies in a simple two-state system under the action of a coupling field: the interaction $\Omega(t)$ always induces repulsion between the energies since the splitting between them is $\sqrt{\Omega^2(t)+\Delta^2(t)}$. In our three-state system, the pump pulse causes repulsion between the energies of states 1 and 2 (the top two energies in Fig. 4, middle frames) and barely influences the energy of state 3. Hence, if the pump pulse is strong enough (which is required for adiabaticity) and the Stokes is weak or absent, the energy of the intermediate adiabatic state $\Phi_2(t)$ (which is the AT state) can approach the lowest adiabatic energy of state $\Phi_3(t)$ (creating an avoided crossing), which will increase the probability for nonadiabatic transitions from state $\Phi_2(t)$ to $\Phi_3(t)$. Likewise, the Stokes pulse applied at the crossing t_{23}^- causes repulsion between the energies of states 2 and 3 and does not affect markedly the energy of state 1. Consequently, the energy of the AT state $\Phi_2(t)$ can approach the energy of the upper adiabatic state $\Phi_1(t)$ with ensuing nonadiabatic losses. Nonadiabatic transitions in these two regions produce nonneglible transient population of state 2 (lower left frame).

This picture is altered significantly when the pump and Stokes pulses exchange their positions, when the Stokes arrives slightly before its crossing at t_{23}^-, whereas the pump pulse arrives somewhat after its crossing at t_{12}^-. For example, the right frames in Fig. 4 display such a case: the pump pulse

is applied at the Stokes's crossing t_{23}^- and the Stokes pulse is applied at the pump's crossing t_{12}^-. Then around t_{12}^- the pump field is still large enough to open up the crossing between states 1 and 2 and make it adiabatic, while at the same time the Stokes pulse is strong enough to push the energy of the adiabatic state $\Phi_3(t)$ away, so that no avoided crossing between $\Phi_2(t)$ and $\Phi_3(t)$ is formed. Similarly, around the second crossing at time t_{23}^- the Stokes pulse opens up the crossing of states 2 and 3 and makes it adiabatic, whereas the action of the pump pulse pushes the uppermost energy of state $\Phi_1(t)$ away and prevents an avoided crossing between $\Phi_1(t)$ and $\Phi_2(t)$. As a result, a smooth transfer of population from state 1 to state 3 occurs, with very small transient population in the decaying state 2.

One can estimate the conditions that minimize the population of state 2 by analyzing the components of the AT state $\Phi_2(t)$, which connects states 1 and 3, and corresponds to the middle eigenenergy in Fig. 4. The condition $P_2 \ll P_1 + P_3$ translates into [see Eq. (19)]

$$\frac{P_1(t)+P_3(t)}{P_2(t)} = \frac{\Omega_p^2(t)}{4\varepsilon_2^2(t)} + \frac{\Omega_s^2(t)}{4[\varepsilon_2(t)-\Delta_3]^2} \gg 1. \qquad (27)$$

Near the crossings t_{12}^- and t_{23}^- we have $\varepsilon_2(t) \sim \Delta_3/2$ and thence in the range (t_{12}^-, t_{23}^-) we should have

$$\frac{P_1(t)+P_3(t)}{P_2(t)} \approx \frac{\Omega_p^2(t)+\Omega_s^2(t)}{\Delta_3^2} \gg 1. \qquad (28)$$

The conclusions derived for the considered arrangement of detunings and pulse timing in this section (case I) extend readily to the alternative arrangement (case II), when the detunings satisfy condition (23b) and the pump and Stokes pulses both follow the Stark pulse. By careful examination of the eigenenergies one can derive similar conclusions regarding the pulse timing: for the minimization of $P_2(t)$ the pump pulse has to be applied at the Stokes's crossing t_{23}^+ and the Stokes pulse at the pump's crossing t_{12}^+. Here again, the Stokes pulse has to precede the pump pulse because $t_{12}^+ < t_{23}^+$. For the sake of brevity, we shall consider below only case I.

The fact that the transient population $P_2(t)$ of state 2 is minimized when the Stokes pulse precedes the pump pulse is reminiscent of STIRAP; however, the reason is quite different, as discussed above. Further discussion and comparison of three-state SCRAP and STIRAP is presented in Sec. V.

IV. PROPERTIES OF THREE-STATE SCRAP

A. Sensitivity to pulse timings

Figure 5 shows contour plots of the final target-state population P_3 as a function of the Stokes position τ_s and the pump position τ_p. The upper frame presents results in the absence of loss, while the lower frame is with loss from state 2.

In the upper frame we see two regions having high transfer probability. The region on the left corresponds to pump and Stokes pulses both applied during the rising of the Stark pulse (three-state SCRAP, case I), whereas the region on the right corresponds to the pulse ordering pump-Stark-Stokes (sequential double SCRAP). In the absence of losses these two regions have almost equal shapes and areas. The adiabatic conditions (25), marked by arrows, describe very accurately the high-efficiency regions. The restrictions imposed by the diabatic conditions (26) are too weak and cannot be seen here.

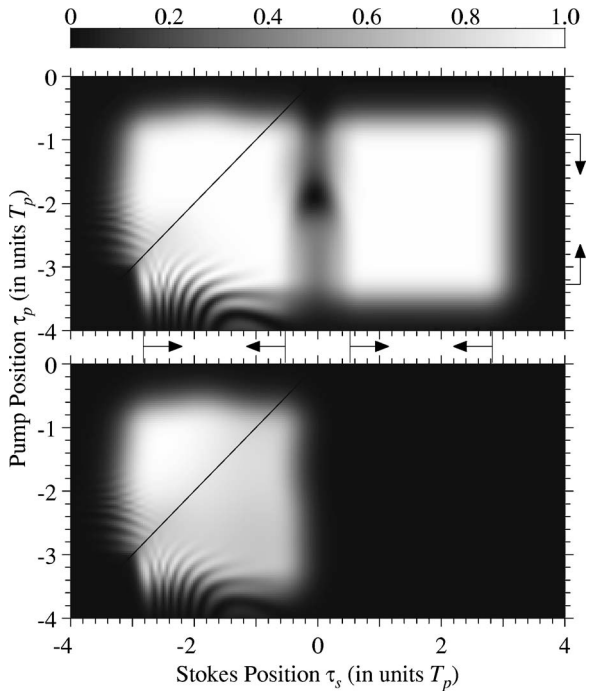

FIG. 5. Contour plots of the final target-state population P_3 as a function of the timings of the pump and Stokes pulses τ_p and τ_s. Upper frame: no decay from state 2, $\Gamma=0$; lower frame: decay from state 2 with rate $\Gamma=1/T_p$. The diagonal line marks the locus of coincident pulses; counterintuitive pulse orderings are to the left of this line. The arrows alongside the axes indicate the parameter ranges where, according to Eqs. (25), the probability should exceed 0.9. The other parameters are $\Delta_2=100/T_p$, $\Delta_3=-50/T_p$, $S_0=300/T_p$, $\Omega_0=50/T_p$, $T=2T_p$, $T_s=T_p$.

The lower frame of this figure shows the effect of irreversible loss from state 2 out of the system. Comparison of the upper and lower frames shows the difference between three-state SCRAP and sequential double SCRAP. The region of high probability associated with sequential double SCRAP disappears in the presence of losses, because the population transfer proceeds through the lossy intermediate state 2. The region on the left, which is associated with three-state SCRAP, is changed less dramatically. The transfer efficiency in the part below the diagonal line, corresponding to the intuitive pulse order pump-Stokes, decreases; however, the transfer efficiency in the part above the diagonal line, corresponding to the counterintuitive pulse order Stokes-pump, is barely changed. The reason is that, as shown in Fig. 4, for the Stokes-pump order state 2 acquires much smaller transient population than for the pump-Stokes order.

To conclude, the three-state SCRAP can transfer population from state 1 to state 3 without placing sizeable transient population into state 2, a feature reminiscent of STIRAP. This suggests that three-state SCRAP can be implemented

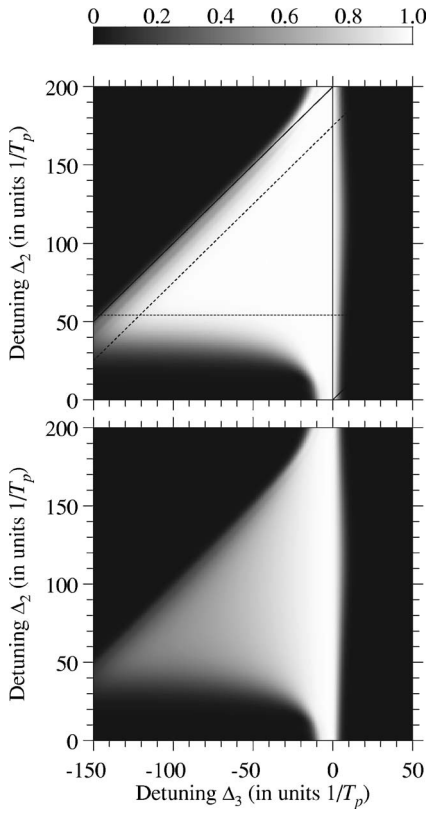

FIG. 6. Contour plots of the final target-state population P_3 as a function of the static detunings Δ_2 and Δ_3. Upper frame: no decay from state 2, $\Gamma=0$; lower frame: decay from state 2 with rate $\Gamma=1/T_p$. The pulses are ordered counterintuitively, with $\tau_p=-T_p$, $\tau_s=-2T_p$. The other parameters are $\Omega_0=50/T_p$, $S_0=200/T_p$, $T=2T_p$, $T_s=T_p$. The solid lines show the bounds of Eqs. (23a) and (23b). The dashed lines show the bounds of Eqs. (25).

even on time scales comparable to the lifetime of state 2. However, SCRAP is not as perfect as STIRAP because some population, albeit small, does visit state 2, whereas in STIRAP this state remains completely unpopulated in the adiabatic limit. Hence some population will be lost in three-state SCRAP if the lifetime of state 2 is shorter than the pulse durations.

B. Sensitivity to detunings

Figure 6 shows contour plots of the final-state population P_3 as a function of the detunings Δ_2 and Δ_3. Detunings can arise both from fluctuations in the laser frequencies as well as from variations in the transition frequency by inhomogeneous broadenings, e.g., Doppler shifts. The pump and Stokes pulses appear in counterintuitive ordering (Stokes-pump), during the rising of the Stark pulse (case I). In the upper frame there is no loss from state 2, while in the lower frame there is irreversible loss. In both cases high population transfer efficiency is localized in one distinct triangular region, corresponding to three-state SCRAP. The analytic conditions, depicted by lines, describe very well the high-efficiency region. In the presence of loss from state 2 this region shrinks, but it is still possible to achieve good population transfer for smaller Δ_3 because, as follows from condition (28), the transient population of the lossy state 2 is smaller for smaller Δ_3. Near two-photon resonance ($\Delta_3=0$) one finds a vertical band of high transfer efficiency, resilient to losses, which is identified with STIRAP.

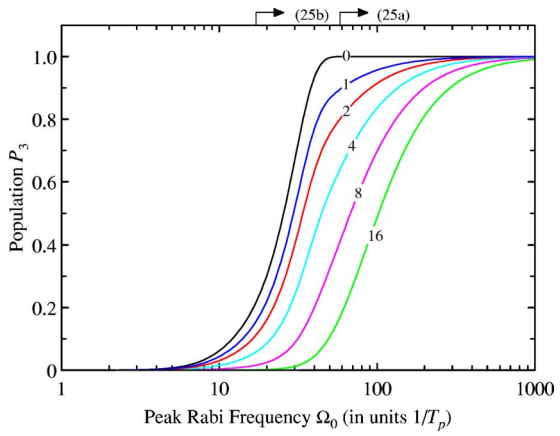

FIG. 7. (Color online) Final target-state population P_3 as a function of the peak Rabi frequency Ω_0. The numbers on the curves denote the rate of population loss from state 2 (in units $1/T_p$). The other parameters are $S_0=200/T_p$, $\Delta_2=100/T_p$, $\Delta_3=-50/T_p$, $\tau_p=-T_p$, $\tau_s=-2T_p$, $T=2T_p$, $T_s=T_p$. The arrows show the adiabatic conditions (25a) and (25b) for $\nu=0.1$. The diabatic conditions (26) require $\Omega_0 T_p < 1.5\times 10^5$ and cannot be seen here.

C. Sensitivity to Rabi frequency

Figure 7 shows the final target-state population P_3 versus the peak Rabi frequencies Ω_0 for several values of the loss rate from state 2 (denoted by numbers on the curves). The detunings and the pulse timings are chosen to satisfy the conditions for case I of three-state SCRAP, when the detunings satisfy condition (23a) and the pump and Stokes pulses are applied during the rising of the Stark pulse. The pump and Stokes pulses appear in counterintuitive ordering (Stokes pump). For sufficiently large Rabi frequency the population transfer efficiency approaches unity for any value of the loss rate; for larger Γ larger Ω_0 is required. The adiabatic conditions (25) are seen to predict very well the high-efficiency region in the lossless case ($\Gamma=0$). From this value on, the population transfer is very robust to variations of the Rabi frequency, as indicative of three-state SCRAP. The stability of the population transfer efficiency versus variations in the Rabi frequency is particularly important for experimental implementations when both intensity fluctuations and averaging over the spatial intensity distribution of the driving radiation fields have to be considered.

V. TWO-PHOTON TRANSITIONS: STIRAP, STIHRAP, AND SCRAP

So far we have assumed that the Stark shifts of levels 1 and 3 are negligible compared to the Stark shift of state 2. We have also assumed that the pump and Stark pulses cause no Stark shifts at all, which is a relevant assumption for single-photon transitions only. In this section we will explore

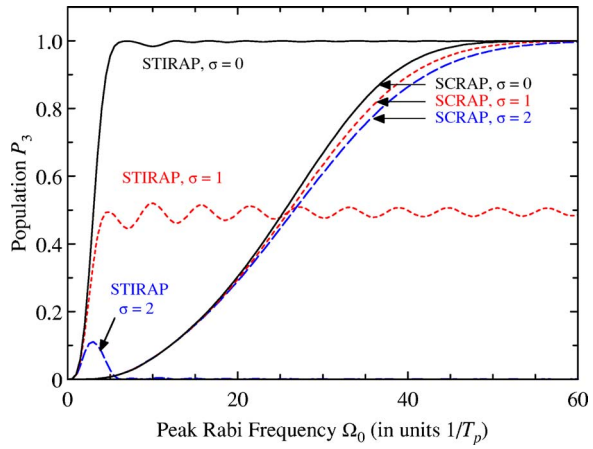

FIG. 8. (Color online) Final target-state population P_3 vs the peak Rabi frequency Ω_0 for STIRAP ($S_0=0$, $\Delta_2=\Delta_3=0$) and three-state SCRAP ($S_0=200/T_p$, $\Delta_2=50/T_p$, $\Delta_3=-25/T_p$). Three cases of different pump-induced Stark shift $S_{31}^p(t)=\sigma\Omega_p(t)$ of state 3 with respect to state 1 are shown with $\sigma=0$, 1, and 2. For all cases the other interaction parameters are $\tau_p=-T_p$, $\tau_s=-2T_p$, $T=2T_p$, $T_s=T_p$, $\Gamma=0$.

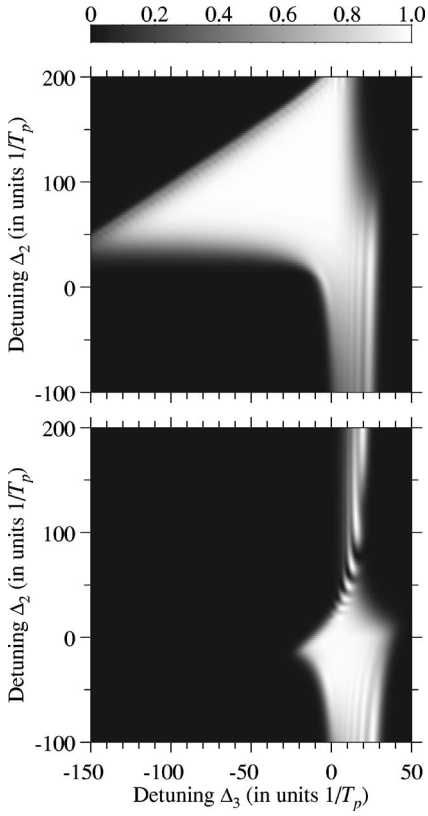

FIG. 9. Contour plots of the final target-state population P_3 as a function of the detunings Δ_2 and Δ_3 in the absence of decay from state 2, $\Gamma=0$. The pulses are ordered counterintuitively, with $\tau_p=-T_p$, $\tau_s=-2T_p$. The other parameters are $\Omega_0=50/T_p$, $T=2T_p$, $T_s=T_p$. Upper frame: $S_0=200/T_p$ (SCRAP); lower frame: $S_0=0$ (STIHRAP).

the effects of Stark shifts caused by the pump pulse as will occur for a two-photon transition. To be specific, we shall consider the hyper-Raman process wherein states 1 and 2 are coupled by a two-photon transition. In this case both the pump-induced Stark shifts $S_{21}^p(t)$ and $S_{31}^p(t)$ and the pump Rabi frequency $\Omega_p(t)$ are proportional to the pump laser intensity.

A. SCRAP vs STIRAP

Laser-induced Stark shifts are recognized as the main obstacle for using STIRAP with two-photon and multiphoton transitions. These shifts, induced by the pump or/and Stokes lasers, change the energy diagram qualitatively by destroying the two-photon resonance and inducing time-dependent two-photon detuning. Such a detuning, if caused by imperfect laser frequency tuning, can in principle be overcome by increasing the laser intensities. The pump- or Stokes-induced Stark shifts, however, are tied to the corresponding Rabi frequency, which cannot be increased independently. Because these Stark shifts are usually comparable to or larger than the respective Rabi frequency, they can prevent the population transfer.

Figure 8 demonstrates these features. Here plots of the final target-state population P_3 are shown as a function of the peak Rabi frequency Ω_0 for three choices of the Stark shift S_{31}^p caused by the pump pulse, which destroys the two-photon resonance. The Stark shift S_{21}^p is less significant and it is taken to be zero. Figure 8 shows that for single-photon transitions ($S_{31}^p=0$) STIRAP is superior as it requires far less intensity. However, for SCRAP the pump-induced Stark shift changes only slightly the transfer efficiency as long as it is smaller than the main Stark shift, induced by the Stark pulse. In contrast, for STIRAP the pump-induced Stark shifts are detrimental and ruin the population transfer. Figure 8 therefore reveals a crucial advantage of SCRAP over STIRAP: SCRAP can be used with multiphoton transitions, despite the induced additional Stark shifts. The reason is that the pump-induced Stark shifts, as long as they are small compared to those produced by the Stark pulse, modify only slightly the energy diagram in SCRAP and do not change it qualitatively; hence the population transfer is not affected significantly. Moreover, the Stark-induced Stark shifts can always be increased independently to diminish the effect of the pump-induced Stark shifts.

B. SCRAP vs STIHRAP

It has been suggested [7] that the detrimental effects of dynamic Stark shifts in STIRAP can be compensated to some extent by a suitable choice of static detunings, via stimulated hyper-Raman adiabatic passage STIHRAP). Indeed, successful coherent population transfer via STIHRAP has been demonstrated experimentally in Ref. [8]. That work has achieved a transfer efficiency of about 50% because of averaging over the spatial profile of the pump laser. The experiments [8]

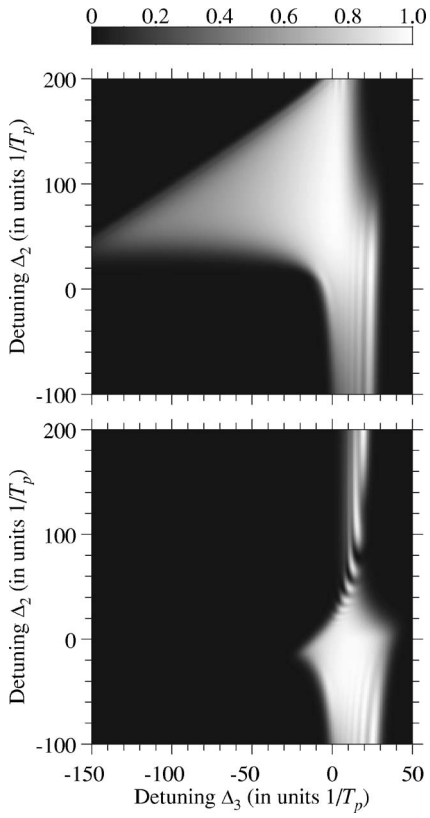

FIG. 10. The same as Fig. 9, but for decayng state 2, with loss rate $\Gamma = 1/T$.

have shown that practical applications of STIHRAP are difficult because the optimal static detunings are very sensitive to the intensity of the pump laser: power variations across the pump-laser beam are detrimental and have to be avoided in order to achieve uniform excitation across the molecular beam. Therefore, to minimize intensity variations in the interaction region it is necessary to work with laser beam diameters substantially larger than the diameter of the molecular beam, which implies that high pulse energies are necessary to saturate the two-photon transition.

Figure 9 shows the final target-state population P_3 as a function of the detunings Δ_2 and Δ_3 for the cases of SCRAP (upper frame) and STIHRAP (lower frame). Figure 10 shows the same plots in the case when state 2 decays out of the system: this figure provides the opportunity to identify the ranges of detunings where the lossy intermediate state 2 gets little transient population and high transfer efficiency persists. Both Figs. 9 and 10 show that high transfer efficiency can be achieved by both SCRAP and STIHRAP. Comparison of the upper and lower frames in Figs. 9 and 10 suggests that SCRAP is more robust than STIHRAP against parameter variations in the presence of unwanted Stark shifts, because of the level-crossing nature of the transition mechanism. This advantage of SCRAP over STIHRAP is very pronounced in the absence of losses (Fig. 9), whereas with losses the two techniques tend to deliver similar results.

VI. CONCLUSIONS

In this paper we have proposed and analysed the extension of the SCRAP technique to three states. The straightforward extension to a sequential double-SCRAP ($1 \rightarrow 2 \rightarrow 3$), consisting of two consecutive single SCRAP processes $1 \rightarrow 2$ and $2 \rightarrow 3$, places all population in the intermediate state 2 for some time; hence SCRAP has to be completed on a time scale shorter than its lifetime. We have found that this problem can be resolved by a genuine three-state SCRAP process, in which all three states are coupled simultaneously and which requires three laser pulses: nearly resonant pump and Stokes, and far-off-resonant Stark-shifting laser. The pump and Stokes pulses have to be both applied during the rising edge of the Stark pulse; then the detunings have to satisfy condition (23a). Alternatively, the pump and Stokes pulses can be applied during the falling edge of the Stark pulse; then the detunings have to satisfy condition (23b). In both cases, population can be transferred coherently, efficiently and robustly from state 1 to state 3, with very little transient population in state 2 at any time.

There are many examples of successful population transfer using chirped frequency lasers and adiabatic rapid passage [5,12], and one might well ask for a comparison of such techniques with the present proposed technique. The use of a frequency chirped laser is always an appropriate choice if the chirp is easy to implement, as is the case with picosecond or femtosecond pulses [12]. However, the adiabaticity criterion, needed for the rapid adiabatic passage, demands a large product of Rabi frequency and interaction time. This is usually more readily accomplished with longer pulses, e.g., nanosecond pulses. However, with such long pulses it is difficult to produce the needed frequency chirp, because their bandwidths are too small to permit methods based on dispersion. Thus the technique described here is advantageous for longer pulses.

Our results suggest that three-state SCRAP can be a powerful alternative of the well-known technique of STIRAP. The main advantage of SCRAP over STIRAP-based techniques is that SCRAP can be used with multiphoton transitions. Such transitions are always accompanied by laser-induced ac Stark shifts that modify the transition frequencies. For STIRAP, such time-dependent shifts are detrimental because they destroy the two-photon resonance, which is crucial for the population transfer. In SCRAP, the Stark shifts are less harmful because, as a level-crossing technique, it does not require maintaining a resonance condition.

We conclude that SCRAP should be superior to STIRAP in media involving multiphoton transitions and inhomogeneous broadenings. For example, in most molecules the first electronically excited levels are typically located more than 5 eV above the vibronic ground level. The excited levels cannot be reached by single-photon transitions, driven by laser systems in the visible or ultraviolet spectral regime. Three-state SCRAP has the potential to provide an efficient tool for coherent population transfer in such cases via multiphoton transitions.

ACKNOWLEDGMENTS

This work has been supported by the European Union's Transfer of Knowledge project CAMEL (Grant No. MTKD-CT-2004-014427), Max-Planck Forschungspreis 2003, Deutsche Forschungsgemeinschaft, and the Alexander von Humboldt Foundation. A.A.R. acknowledges support from the EU Marie Curie Training Site Project No. HPMT-CT-2001-00294.

[1] L. P. Yatsenko, B. W. Shore, T. Halfmann, K. Bergmann, and A. Vardi, Phys. Rev. A **60**, R4237 (1999).

[2] T. Rickes, L. P. Yatsenko, S. Steuerwald, T. Halfmann, B. W. Shore, N. V. Vitanov, and K. Bergmann, J. Chem. Phys. **115**, 534 (2000).

[3] T. Rickes, J. P. Marangos, and T. Halfmann, Opt. Commun. **227**, 133 (2003).

[4] L. P. Yatsenko, N. V. Vitanov, B. W. Shore, T. Rickes, and K. Bergmann, Opt. Commun. **204**, 413 (2002).

[5] N. V. Vitanov, T. Halfmann, B. W. Shore, and K. Bergmann, Annu. Rev. Phys. Chem. **52**, 763 (2001); N. V. Vitanov, M. Fleischhauer, B. W. Shore, and K. Bergmann, Adv. At., Mol., Opt. Phys. **46**, 55 (2001).

[6] E. Arimondo, Prog. Opt. **35**, 259 (1996).

[7] L. P. Yatsenko, S. Guerin, T. Halfmann, K. Bohmer, B. W. Shore, and K. Bergmann, Phys. Rev. A **58**, 4683 (1998); S. Guerin, L. P. Yatsenko, T. Halfmann, B. W. Shore, and K. Bergmann, Phys. Rev. A **58**, 4691 (1998).

[8] K. Bohmer, T. Halfmann, L. P. Yatsenko, B. W. Shore, and K. Bergmann, Phys. Rev. A **64**, 023404 (2001).

[9] B. W. Shore, *The Theory of Coherent Atomic Excitation* (Wiley, New York, 1990).

[10] A. Kuhn, H. Perrin, W. Hänsel, and C. Salomon, in *OSA TOPS on Ultracold Atoms and BEC*, edited by K. Burnett (Optical Society of America, Washington, D. C., 1996), Vol. 7, p. 58.

[11] C. Zener, Proc. R. Soc. London, Ser. A **137**, 696 (1932).

[12] J. S. Melinger, A. Hariharan, S. R. Gandhi, and W. S. Warren, J. Chem. Phys. **95**, 2210 (1991); J. S. Melinger, S. R. Gandhi, A. Hariharan, D. Goswami, and W. S. Warren, *ibid.* **101**, 6439 (1994); J. S. Melinger, D. McMorrow, C. Hillegas, and W. S. Warren, Phys. Rev. A **51**, 3366 (1995); J. C. Davis and W. S. Warren, J. Chem. Phys. **110**, 4229 (1999).